Physics Letters A 379 (2015) 1172–1177

Contents lists available at ScienceDirect

Physics Letters A

www.elsevier.com/locate/pla

Characteristics of the conductance in ferromagnet/spin-triplet superconductor junctions with helical p-wave states

Qiang Cheng [a,*], Biao Jin [b], Dongyang Yu [c]

[a] School of Science, Qingdao Technological University, Qingdao 266520, China
[b] School of Physics, University of Chinese Academy of Sciences, Beijing 100049, China
[c] Department of Physics, Renmin University of China, Beijing, China

ARTICLE INFO

Article history:
Received 2 December 2014
Received in revised form 26 January 2015
Accepted 10 February 2015
Available online 12 February 2015
Communicated by R. Wu

Keywords:
Tunneling conductance
Ferromagnet
Spin-triplet superconductor
Helical p-wave states

ABSTRACT

We study the charge conductance in ferromagnet/spin-triplet superconductor junctions with the helical superconducting states, $k_x\hat{x} \pm k_y\hat{y}$ or $k_y\hat{x} \pm k_x\hat{y}$, which are consistent with the in-plane $H_{c2,ab}$ measurements of Sr_2RuO_4. The conductance shows strong anisotropic dependence on the orientation of the magnetization in ferromagnet and is simultaneously symmetric about some specific rotations. The effects of the magnetization magnitude and the height of the interfacial barrier are also investigated. The obtained results may provide helpful information about the pairing symmetries in Sr_2RuO_4.

1. Introduction

The layered perovskite oxide Sr_2RuO_4 is believed to be a rare example of spin-triplet superconductor (TS) [1], which was discovered by Maeno et al. [2]. The Cooper pair wave function in TS can be described with the three-component complex **d**-vector [3]. The determination of the exact form of the vector in Sr_2RuO_4 has attracted a large number of experimental and theoretical researches [1,4]. Unfortunately, the obtained results are not yet converged. For example, the experiment on the electronic spin susceptibility indicates the **d**-vector is parallel to the crystal c-axis, i.e. $\mathbf{d} \parallel \hat{z}$ [5]. The muon spin resonance experiments and the observation of the polar Kerr effect in the superconducting state of Sr_2RuO_4 are consistent with the chiral p-wave state $\mathbf{d}(\mathbf{k}) = (k_x + ik_y)\hat{z}$ [6,7]. However, the Knight-shift measurements and the microscopic calculations devoted to clarify the mechanism of TS as well as the **d**-vector direction in Sr_2RuO_4 support an intrinsic in-plane **d**-vector [8–12]. Further experimental and theoretical efforts seem to be necessary to determine the symmetry and the direction of the vector in Sr_2RuO_4 unambiguously.

Tunneling spectroscopy is a direct and effective probe of the pairing symmetry of superconducting states [13,14]. Especially, the studies on the transport properties in ferromagnet (F)/TS junctions not only provide important information about the **d**-vector but also possess potential applications in spintronics. It is found in Ref. [15] the conductance of F/TS junction with $\mathbf{d} \parallel \hat{z}$ strongly depends on the direction of the magnetization. Spin current and 0–π transition in F/TS and TS/F/TS structures are also studied by Brydon et al. [16,17]. In these structures, the physical mechanism is the interplay between the magnetization and the **d**-vector and its influences on Andreev reflection (AR) [18].

In order to set further restrictions on the pairing symmetry in Sr_2RuO_4, Zhang et al. [19] recently calculate the angular and temperature T dependencies of the upper critical field $H_{c2}(\theta, \phi, T)$ for the helical p-wave states

$$\mathbf{d}(\mathbf{k}) = \Delta(\hat{x}k_x \pm \hat{y}k_y) \quad \text{or} \quad \Delta(\hat{x}k_y \pm \hat{y}k_x) \tag{1}$$

and find good fits to the Sr_2RuO_4 $H_{c2,a}(\theta, T)$ data of Kittaka et al. [20]. They further point out that the chiral p-wave state and the Scharnberg–Klemm state [21] are inconsistent with the $H_{c2,a}(\theta, T)$ data. The transport properties in normal metal (N)/TS and non-centrosymmetric superconductors structures relating to helical states have also been investigated [22,23]. However, the interactions of magnetization and the helical states and their influences on the charge transport is still unclear. Our motivation in this paper is to clarify the magnetization dependence of the charge conductance in F/TS junction assuming the superconducting states presented in Eq. (1). For simplicity, we restrict ourselves to the case of a cylindrical Fermi surface in TS. We find when the magnetization in F is rotated, the conductance shows strong anisotropy and is simultaneously symmetric about specific rotations. The re-

* Corresponding author.
E-mail address: chengqiang07@mails.ucas.ac.cn (Q. Cheng).

http://dx.doi.org/10.1016/j.physleta.2015.02.015
0375-9601/

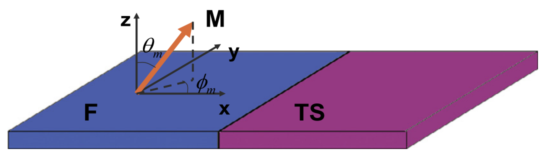

Fig. 1. Schematic illustration of ferromagnet (F)/spin-triplet superconductor (TS) junction with the helical states. The **d**-vector in TS is in *xoy* plane and its direction is dependent on the wavevector **k**. The direction of the magnetization in F is denoted by the polar angle θ_m and the azimuthal angle ϕ_m. The current in the junction is flowing along the x-axis.

sults are distinct from that in F/TS junctions with chiral p-wave state where the conductance is a cosine function of the relative angle between the magnetization and **d**-vector [24]. For clarity, we discuss the zero bias conductance (ZBC) as a function of the polar angle and the azimuthal angle of the magnetization. The effects of the magnetization magnitude and the interface barrier are also investigated.

2. Model and formalism

We consider an F/TS junction as shown in Fig. 1. The interface barrier, located at $x=0$ and along y axis, is modeled by a delta function $U(x)=U\delta(x)$. The effective Hamiltonian $\check{H}$ of the junction for the Bogoliubov–de Gennes (BdG) equation $\check{H}\Psi=E\Psi$ is expressed as

$$\check{H}=\begin{pmatrix} \hat{H}(\mathbf{k}) & \hat{\Delta}(\mathbf{k})\Theta(x) \\ -\hat{\Delta}^*(-\mathbf{k})\Theta(x) & -\hat{H}^*(-\mathbf{k}) \end{pmatrix}, \tag{2}$$

where $\hat{H}(\mathbf{k})=\xi_k-\mathbf{M}\cdot\hat{\sigma}\Theta(-x)+U(x)$ with $\xi_k=\frac{\hbar^2k^2}{2m}-E_F$ and $\hat{\sigma}$ the Pauli matrixes. The magnetization $\mathbf{M}=M(\sin\theta_m\cos\phi_m, \sin\theta_m\sin\phi_m,\cos\theta_m)$ with θ_m the polar angle and ϕ_m the azimuthal angle. The energy gap matrix

$$\hat{\Delta}=(\mathbf{d}(\mathbf{k})\cdot\hat{\sigma})i\hat{\sigma}_2 \tag{3}$$

with $\mathbf{d}(\mathbf{k})=\Delta(k_x,\pm k_y,0)$ or $\Delta(k_y,\pm k_x,0)$.

For the spin of electrons, we chose the direction of $\mathbf{M}$ as the quantization axis. Let us consider an electron with majority spin (spin-up) is injected from F. Upon defining $\check{e}_1=(1,0,0,0)^T$, $\check{e}_2=(0,1,0,0)^T$, $\check{e}_3=(0,0,1,0)^T$ and $\check{e}_4=(0,0,0,1)^T$ as the basic vectors in the pair spin space, the wave function in F is expressed as

$$\begin{aligned}\Psi_F(x<0)=&(\chi_1e^{ik_1x}+b_{\uparrow\uparrow}\chi_1e^{-ik_1x}-b_{\uparrow\downarrow}\chi_2^*e^{-ik_2x})\check{e}_1\\ &+(\chi_2e^{ik_1x}+b_{\uparrow\uparrow}\chi_2e^{-ik_1x}+b_{\uparrow\downarrow}\chi_1e^{-ik_2x})\check{e}_2\\ &+(a_{\uparrow\uparrow}\chi_1e^{ik_1x}-a_{\uparrow\downarrow}\chi_2e^{ik_2x})\check{e}_3\\ &+(a_{\uparrow\uparrow}\chi_2^*e^{ik_1x}+a_{\uparrow\downarrow}\chi_1e^{ik_2x})\check{e}_4,\end{aligned} \tag{4}$$

where $\chi_1=\cos\frac{\theta_m}{2}$, $\chi_2=\sin\frac{\theta_m}{2}e^{i\phi_m}$ and $k_{1(2)}=\sqrt{\frac{2m}{\hbar^2}(E_F+(-)M)-k_y^2}$. The coefficients $b_{\uparrow\uparrow}$ $(b_{\uparrow\downarrow})$ and $a_{\uparrow\uparrow}$ $(a_{\uparrow\downarrow})$ represent the normal reflection to majority (minority) spin subband and the AR to majority (minority) spin subband, respectively.

The wave function in TS is given by

$$\begin{aligned}\Psi_{TS}(x>0)=&(c_{\uparrow\uparrow}ue^{ik_xx}-d_{\uparrow\uparrow}v\eta^*(\pi-\theta_s)e^{-ik_xx})\check{e}_1\\ &+(c_{\uparrow\downarrow}ue^{ik_xx}+d_{\uparrow\downarrow}v\eta(\pi-\theta_s)e^{-ik_xx})\check{e}_2\\ &+(-c_{\uparrow\uparrow}v\eta(\theta_s)e^{ik_xx}+d_{\uparrow\uparrow}ue^{-ik_xx})\check{e}_3\\ &+(c_{\uparrow\downarrow}v\eta^*(\theta_s)e^{ik_xx}+d_{\uparrow\downarrow}ue^{-ik_xx})\check{e}_4,\end{aligned} \tag{5}$$

where $c_{\uparrow\uparrow}, c_{\uparrow\downarrow}, d_{\uparrow\uparrow}$ and $d_{\uparrow\downarrow}$ are the transmission coefficients of electron-like quasiparticle and hole-like quasiparticle, respectively, the coherent factors $u(v)=\sqrt{\frac{E+(-)\Omega}{2E}}$ with $\Omega=\sqrt{E^2-\Delta^2}$, the phase factor $\eta(\theta_s)=\frac{d_x+id_y}{|\mathbf{d}(\mathbf{k})|}$ with $(d_x,d_y)=(k_x,\pm k_y)$ or $(k_y,\pm k_x)$ and $k_x\approx k_F\cos\theta_s$ with θ_s the angle between the x-axis and the wavevector of the electron-like quasiparticle in TS and k_F the Fermi wavevector. Due to the momentum conservation along the y axis, the k_y in $k_{\uparrow(\downarrow)}$ and $\mathbf{d}(\mathbf{k})$ can be expressed as $k_F\sin\theta_s$. In our work, we don't take into account the Fermi wavevector mismatch between F and TS.

All the coefficients in the wave functions can be determined under the boundary conditions:

$$\Psi_F(x=0^-)=\Psi_{TS}(x=0^+), \tag{6}$$

$$\Psi'_{TS}(x=0^+)-\Psi'_F(x=0^-)=\frac{2mU}{\hbar^2}\Psi_F(x=0). \tag{7}$$

The reflection and transmission coefficients of an injection electron with the minority spin (spin-down) can be obtained in a similar way.

According to the Blonder–Tinkham–Klapwijk formalism [25], the normalized tunneling conductance σ can be written as

$$\sigma=\frac{\int(\sigma_\uparrow+\sigma_\downarrow)\cos\theta_s d\theta_s}{\sigma_N}, \tag{8}$$

with

$$\sigma_\uparrow=\frac{1+X}{2}(1+|a_{\uparrow\uparrow}|^2+\frac{k_2}{k_1}|a_{\uparrow\downarrow}|^2-|b_{\uparrow\uparrow}|^2-\frac{k_2}{k_1}|b_{\uparrow\downarrow}|^2), \tag{9}$$

$$\sigma_\downarrow=\frac{1-X}{2}(1+|a_{\downarrow\downarrow}|^2+\frac{k_1}{k_2}|a_{\downarrow\uparrow}|^2-|b_{\downarrow\downarrow}|^2-\frac{k_1}{k_2}|b_{\downarrow\uparrow}|^2), \tag{10}$$

and σ_N the conductance for F/N junction. In the calculation of the integral we have considered the presence of the critical angle $\theta_C=\arcsin\sqrt{1-X}$ and the virtual AR process [26]. For a given bias V, the conductance σ is a function of the polar angle θ_m, the azimuthal angle ϕ_m, the magnitude of the magnetization $X=\frac{M}{E_F}$ and the interface barrier heights $Z=\frac{2mU}{\hbar^2k_F}$.

3. Results and discussions

We first discuss some general consequences concerning the conductance. (1) The states $\hat{x}k_x\pm\hat{y}k_y$ (or $\hat{x}k_y\pm\hat{y}k_x$) possess the same conductance spectra. As a result, one can't distinguish between the sates $\hat{x}k_x\pm\hat{y}k_y$ (or $\hat{x}k_y\pm\hat{y}k_x$) by means of the tunneling experiments. (2) The conductance for both $\hat{x}k_x+\hat{y}k_y$ and $\hat{x}k_y+\hat{y}k_x$ are symmetric about the magnetization orientation: $\sigma(\theta_m,\phi_m)=\sigma(\theta_m,\pi+\phi_m)$ and $\sigma(\theta_m,\phi_m)=\sigma(\pi-\theta_m,\pi-\phi_m)$, which can be deduced directly from the analytic expressions for the reflection coefficients (see Appendix A). (3) Although the conductance for (θ_m,ϕ_m) is different from that for $(\pi-\theta_m,\phi_m)$, there is only a slight difference between them. Due to the above features, we only consider the conductance for the angle interval $0\le\theta_m\le\pi/2$ and $0\le\phi_m\le\pi/2$ in our numerical results.

3.1. F/$(\hat{x}k_x\pm\hat{y}k_y)$ junction

Fig. 2 gives the conductance spectra at $X=0.9$ and $Z=0$ with $\phi_m=0, 0.3\pi$ and 0.5π. For each ϕ_m, $\theta_m=0, 0.3\pi$ and 0.5π are considered. When $\theta_m=0$, the magnetization is perpendicular to $\mathbf{d}(\mathbf{k})$ for all $\mathbf{k}$. In this case, the subgap conductance is not suppressed sharply by the spin-polarization in F, which is a similar characteristic to the conductance in F/chiral p-wave TS junction with a uniform **d**-vector. When $\theta_m\neq0$, the subgap conductance show a strong dependence on ϕ_m. As one increases ϕ_m, the ZBC for $\theta_m=0.3\pi$ is enhanced while that for $\theta_m=0.5\pi$ has a non-monotonic behavior. Fig. 3 presents the spectra for $X=0.9$ and